**Title:** Can hydraulic design explain patterns of leaf water isotopic enrichment in $C_3$ plants?

**Running Head:** Leaf hydraulic design and water isotopes

**Authors:** Margaret M. Barbour[1,2], Karen E. Loucos[1], Erin L. Lockhart[1], Arjina Shrestha[1], Daniel McCallum[1], Kevin A. Simonin[3], Xin Song[4], Danielle S. Griffani[5] and Graham D. Farquhar[5],

**Affiliations:**

[1]The University of Sydney, School of Life and Environmental Sciences, NSW 2570, Australia

[2]The University of Waikato, School of Science, Hamilton 3240, New Zealand

[3]Department of Biology, San Francisco State University, San Francisco, CA, 94132, USA

[4]College of Life Sciences and Oceanography, Shenzhen University, Shenzhen, Guangdong, 518060, People's Republic of China

[5]Research School of Biology, The Australian National University, Canberra, ACT 0200, Australia

**Contact Information:** corresponding author margaret.barbour@sydney.edu.au

## ABSTRACT

$H_2{}^{18}O$ enrichment develops when leaves transpire, but an accurate generalised mechanistic model has proven elusive. We hypothesised that leaf hydraulic architecture may affect the degree to which gradients in $H_2{}^{18}O$ develop within leaves, influencing bulk leaf stable oxygen isotope enrichment ($\Delta_L$) and the degree to which the Péclet effect is relevant in leaves. Leaf hydraulic design predicted the relevance of a Péclet effect to $\Delta_L$ in 19 of the 21 species tested. Leaves with well-developed hydraulic connections between the vascular tissue and the epidermal cells through bundle sheath extensions and clear distinctions between palisade and spongy mesophyll layers (while the mesophyll is hydraulically disconnected) may have velocities of the transpiration stream such that gradients in $H_2{}^{18}O$ develop and are expressed in the mesophyll. In contrast, in leaves where the vascular tissue is hydraulically disconnected from the epidermal layers, or where all mesophyll cells are well connected to the transpiration stream, velocities within the liquid transport pathways may be low enough that gradients in $H_2{}^{18}O$ are very small. Prior knowledge of leaf hydraulic design allows informed selection of the appropriate $\Delta_L$ modelling framework.



**Keywords:** oxygen isotope; leaf water; transpiration; Péclet effect; two-pool model

**Funding**: Australian Research Council DP170104276

**Acknowledgements:** K.E.L. was supported by an Australian Postgraduate Award and A.S. was supported by an Australian Postgraduate Award and International Postgraduate Research Support. Elinor Goodman is thanked for assistance with leaf microscopy. The authors acknowledge the facilities and the scientific and technical assistance of Microscopy Australia at the Australian Centre for Microscopy & Microanalysis at the University of Sydney. The authors have no conflicts of interest to declare.

**Summary sentence:** We show that leaf hydraulic design contributes to the development of gradients in oxygen isotope composition within leaf water, and that *a priori* knowledge of leaf hydraulic design can guide selection of appropriate leaf water isotope models.

**Author contributions:** M.M.B. and K.E.L co-designed the experiment; M.M.B., K.E.L., E.L.L., A.S., and D.M. conducted the experiment. M.M.B. and K.E.L. drafted the manuscript and all authors contributed to interpretation of data, writing and editing of the manuscript.

## INTRODUCTION

The stable oxygen isotope composition of leaf water is at the crossroads of a number of important aspects of global cycles of carbon and water: leaf water influences the oxygen isotope composition of both $O_2$ and $CO_2$, and so is used to determine terrestrial versus oceanic productivity (the "Dole effect": Dole et al. 1954; Bender, Sowers and Labeyrie, 1994) and to constrain global carbon models (e.g. Ciais et al. 1997; Welp et al. 2011). Further, leaf water

imparts an isotopic signal on plant organic material that has been exploited to reconstruct past climates from tree rings (Libby et al. 1979), to interpret plant regulation of water loss (Barbour 2007) and to predict assimilation-weighted leaf temperature (Helliker and Richter 2008). Given this range in applications there is an urgent need to understand the factors controlling measured variation in leaf water oxygen isotope composition ($\Delta_L$) and to build mechanistic models for the prediction of $\Delta_L$ in time and space. The contradictory evidence in the literature regarding the accuracy of various modelling approaches is impeding progress (Cernusak et al. 2016).

The most widely applied model for characterising the enrichment of $H_2{}^{18}O$ at the sites of evaporation relative to source water ($\Delta_e$), the Craig-Gordon model (Craig and Gordon 1965), was developed for evaporation from open bodies of water and subsequently adapted to plants (Dongmann et al. 1974; Flanagan, Comstock and Ehleringer 1991). However, it was demonstrated thereafter that this model tends to over-estimate $\Delta_e$ compared to measured bulk leaf water (Flanagan, Comstock and Ehleringer 1991). One option to account for the discrepancy between $\Delta_e$ and $\Delta_L$ is with a discrete-pool model, which considers bulk leaf water as a mixture of pools of water (Leaney et al. 1985; Yakir, DeNiro and Rundel, 1989). The simplest form of this model is the two-pool model, where bulk leaf water is separated into two isotopically distinct pools, one in the lamina and the second in the veins. However, some measurements suggested that the difference between $\Delta_e$ and $\Delta_L$ scaled with transpiration rate (Walker et al. 1989), a trend the two-pool model does not predict (Barbour et al. 2000). An alternative leaf water model was proposed, which describes the formation of isotopic gradients within leaves as a Péclet effect that occurs as the backward diffusion of heavy water isotopologues (i.e. $H_2{}^{18}O$) is opposed by bulk water flow to the sites of evaporation (Farquhar and Lloyd 1993). Implicit within Péclet effect theory is a positive relationship between transpiration rate and the fractional difference between

83 $\Delta_e$ and $\Delta_L$ under steady state conditions ($1-\Delta_L/\Delta_e$; Farquhar and Lloyd 1993). The two different
84 modelling approaches require either extensive data collection to assess different models or an *a*
85 *priori* knowledge of the most appropriate model.

86 We propose that leaf hydraulic architecture can be used to inform the choice of stable isotope
87 models of bulk leaf water. The relative contribution of apoplastic, symplastic and transcellular
88 pathways (Steudle, Murrmann and Peterson, 1993; Aasamaa, Niinemets and Sober, 2005) to the
89 transpiration flux and how they interact is predicted to influence the development of gradients in
90 enrichment within leaves, and hence the isotope composition of bulk leaf water (Barbour and
91 Farquhar 2003). Measurements of whole leaf rehydration kinetics provide evidence of hydraulic
92 compartmentalisation, with leaves falling into three different *hydraulic designs* (Zwieniecki,
93 Brodribb and Holbrook, 2007):

94 Design 1: relatively weak hydraulic connections (i.e. high resistance) between veins, mesophyll
95 and epidermal cells

96 Design 2: veins and epidermal cells are well connected hydraulically but the contribution of
97 mesophyll cells to transpiration is relatively restricted due to high hydraulic resistance

98 Design 3: all tissues are hydraulically well connected.

99 The aim of the following study was to examine how hydraulic design may be used to explain
100 patterns of leaf water enrichment at the whole leaf level. We examined 21 $C_3$ species, which
101 were allocated to one of the three hydraulic designs using leaf anatomical properties visible
102 under a light microscope. The relationship between transpiration rate and $1-\Delta_L/\Delta_e$ was quantified
103 to test whether hydraulic design can be used to inform the choice of isotopic model.

## MATERIALS AND METHODS

### Growth Conditions

*Eucalyptus amplifolia* Naud., *Eucalyptus botryoides* Smith, *Eucalyptus camaldulensis* Dehnh., *Eucalyptus globulus* Labill., *Eucalyptus grandis* W. Hill ex Maiden, *Eucalyptus occidentalis* Endl., *Eucalyptus polybractea* R.T. Baker, *Eucalyptus stellulata* Sieber ex DC., *Acer x freemanii* A.E Murray Autumn Blaze (Jeffersred), *Camellia sasanqua* Thunb. cv Paradise Belinda, *Ginkgo biloba* L., *Vitis vinifera* L. cv. Sultana M12 and *Wollemia nobilis* W.G. Jones, K.D. Hill & J.M. Allen. were purchased locally as seedlings. All seedlings except for *C. sasanqua* were placed into larger pots filled with locally purchased soil mix and amended with slow release fertiliser (Osmocote, Scotts Australia Pty Ltd., Sydney, NSW, Australia). *Eucalyptus parramattensis* Hall, *Helianthus annuus* L., *Phaseolus vulgaris* L., *Glycine max* L. Merr, *Gossypium hirsutum* L., *Triticum aestivum* L. cv Cranbrook and *Cicer arietinum* L. (cvs Amethyst, Hattrick and Kyabra) were grown from seed in potting mix amended with slow release fertiliser (Osmocote, Scotts Australia Pty Ltd., Sydney, NSW, Australia).

*P. vulgaris*, *G. max*, *T. aestivum* and *C. arietinum* were grown in a controlled environment room at the Centre for Carbon, Water and Food (University of Sydney, Camden NSW, Australia) at a day/night temperature of 25/17ºC, 14 h day period, day and night air humidity of 75% and an approximate irradiance at the top of the canopy of 600 µmol $m^{-2}$ $s^{-1}$. *G. hirsutum* and *H. annuus* (NSS sample batch) were grown in a controlled environment room with a day/night temperature of 28/20ºC, 75% air humidity in the day and night, 14 h day period and an approximate irradiance at the top of the canopy of 600 µmol $m^{-2}$ $s^{-1}$. *H. annuus* (SS sample batch) and *C.*

126 *sasanqua* were grown in a controlled environment room with a day/night temperature of
127 25/20°C, day and night air humidity of 70%, 16 h light period and an approximate irradiance
128 intensity of 700 μmol $m^{-2}$ $s^{-1}$ at the top of the canopy. The *Eucalyptus* species, *Acer x freemanii*
129 and *W. nobilis* (after an initial period of growth in the controlled environment room with the
130 above conditions) were placed into a glasshouse in ambient conditions at the Centre for Carbon,
131 Water and Food. All species were watered daily to maintain soil water at field capacity. Gas
132 exchange measurements were made when the *Eucalyptus*, *Acer x freemanii*, *W. nobilis* and *C.*
133 *sasanqua* seedlings were 6 months-4 years old and 4-8 weeks after germination for the rest of the
134 species.

135 Five genotypes of *Vicia faba* L. (PBA Rana, Cairo, PBA Warda, Doza and 220d) were grown
136 from seed under four different $CO_2$ and irradiance environmental conditions inside two growth
137 environment rooms. The rooms were set to a day/night temperature of 25/17ºC, 75% air
138 humidity and a $CO_2$ partial pressure of either 60.4 or 100.7 Pa. Differences in irradiance were
139 imposed by covering half of the plants with shade cloth, which reduced irradiance from 600 to
140 200 μmol $m^{-2}$ $s^{-1}$. Plants were watered daily and measured when they were approximately 6
141 weeks old.

142

143 Gas exchange and isotope measurements

144 Gas exchange was recorded at one minute intervals on a LiCor portable photosynthesis system
145 (Li6400xt, LiCor Inc., Lincoln, NE, USA) fitted with either a custom-built large leaf chamber
146 (leaf area of 38 $cm^2$; Loucos et al. 2015), 2 x 6 cm chamber (Li6400-11; LiCor Inc.) or standard
147 2 x 3 cm chamber with a red-blue LED irradiance source (Li6400-02B; LiCor Inc.). For the two

larger chambers a red-green-blue irradiance source was used (Li6400-18A; LiCor Inc.), which had a maximum red-blue irradiance intensity of 1300 μmol $m^{-2}$ $s^{-1}$.

Transpiration rates were varied by manipulating irradiance, $CO_2$ partial pressure, leaf temperature and intercellular-to-atmospheric vapour pressure difference (VPd). Leaf temperature varied between 21.5 and 30.7ºC, $CO_2$ partial pressure between 5.0 and 120.8 Pa (given an atmospheric pressure of 100.7 kPa) and irradiance was varied from 50 to1300 μmol $m^{-2}$ $s^{-1}$. VPd was manipulated by altering flow rate, which was varied between 250 and 710 μmol $s^{-1}$. For the leaves of *V. faba* genotypes only, environmental conditions inside the LiCor chamber were matched to the growth environmental conditions (see above) with a range of VPd between 0.9 and 4.1 kPa.

A subset of *H.annuus*, *E. grandis* and *E. parramattensis* leaves were measured under contrasting irradiance of 200 and 1200 μmol $m^{-2}$ $s^{-1}$ in order to test whether irradiance influences the location of the sites of evaporation (as suggested by Buckley et al. 2017), and consequently the Péclet effective length. For these measurements, transpiration rate was varied through changes in $CO_2$ concentration and flow rate.

Transpiration isotopologues were measured by attaching the LiCor system to a Picarro (L1102-i; Picarro Inc., Sunnyvale, CA, USA) or Los Gatos Research water vapour gas analyser (TIWA-45EP; Los Gatos Inc., Mount View, CA, USA) with the air entering the LiCor chamber completely dried. Drying the ingoing air meant the water vapour concentration exiting the chamber was entirely derived from leaf transpiration. The gas analysers recorded the oxygen isotope ratio every 1-5 s (later converted to minute averages). The youngest, fully expanded leaves were selected and either part or the whole leaf was enclosed in the chamber. Leaves

remained in the chamber until transpiration rates had stabilised but isotopes were still at non-steady state (10 – 60 min; NSS) or the oxygen isotope composition had stabilised and isotopic steady state was assumed (between 40 min and 7 h 20 min; SS), depending on the species.

Once the gas exchange measurements were completed leaves were collected for water extraction or equilibration in three different ways (see Supp. Table 3). For the whole leaf samples of the *Eucalyptus* species, *Acer x freemanii*, *G. biloba*, *V. faba* genotypes, *V. vinifera*, *C. arietinum* genotypes and part leaf samples of *H. annuus* (SS batch, only the leaf area within the chamber), leaves were cut at the end of gas exchange and isotope measurements, photographed for calculation of one-sided leaf area using ImageJ (1.45s, NIH, Bethesda, MD, USA) and the leaves (without the petiole) were sealed in glass vials and stored at -20°C for extraction via vacuum distillation. *C. sasanqua* and *W. nobilis* samples were also prepared as described above except that for these samples, the primary vein and lamina tissue was placed into separate glass vials. For a second set of samples from the *Eucalyptus* species and *Acer x freemanii*, whole leaves were cut at the petiole and then the primary vein and lamina tissue were separated and sealed into separate glass vials flushed with 2% $CO_2$ for direct equilibration. For the remaining species, the section of the leaf inside the chamber was cut away and sealed in a glass vial flushed with 2% $CO_2$ for direct equilibration. An individual sampling method typically took less than two minutes to complete.

The Picarro and LGR analysers were calibrated following the protocol described by Simonin et al. (2013) every 2-7 days during experimentation. A multiple linear regression was performed for each calibration, which included a correction of the raw isotope data for any concentration dependence.

192

193 Leaf water extraction and oxygen isotope analysis

194 For leaf samples stored at -20ºC, leaf water was extracted via the vacuum distillation method
195 (West, Patrickson and Ehleringer, 200). Extracted leaf water was then equilibrated with $CO_2$
196 using the method described by Loucos et al. (2015), while directly-equilibrated leaf samples
197 followed the method described by Song and Barbour (2016) for measurement of leaf water $^{18}O$.
198 All samples were then measured on a tunable-diode laser absorption spectrometer (model
199 TGA100A, Campbell Scientific, Inc., Logan, UT, USA). Values from equilibrated samples were
200 corrected using the general equation for the difference between extracted and directly
201 equilibrated water samples (Song and Barbour 2016).

202

203 The Péclet Effect Model

204 Isotopic enrichment above source water (Δ) was expressed in per mil (‰) as:

205 $$\Delta = \frac{meas}{R_s} - 1, (1)$$

206 where $R_{meas}$ is the measured isotopic ratio ($^{18}O/^{16}O$) of either the atmospheric water vapour,
207 evaporative site water or leaf water, and $R_s$ is the isotopic ratio of the source water (the isotopic
208 composition of transpired vapour was used; Song et al. 2015). Thus calculation of Δ was
209 expressed as ($\delta_{meas}$ is the measured or estimated isotopic composition):

210 $$\Delta = \frac{(\delta_{meas} - \delta_{trans})}{(1+\delta_{trans})}. \qquad (2)$$

The steady-state model of isotopic enrichment at the sites of evaporation ($\Delta_e$) is based on the Craig-Gordon model for evaporation from the surface of water bodies (Craig and Gordon 1965), adapted to plants (Dongmann et al. 1974) and modified for boundary layer effects (Farquhar et al. 1989);

$$\Delta_e = \varepsilon^+ + \varepsilon_k + (\Delta_v - \varepsilon_k)\, {}^{e_a}/_{e_i}, \qquad (3)$$

where $\Delta_v$ is the isotopic enrichment of the water vapour in the leaf chamber, $\varepsilon^+$ and $\varepsilon_k$ the equilibrium and kinetic fractionation factors and $e_a/e_i$ is the ambient to intercellular mole fraction of water vapour. The equilibrium fractionation factor, $\varepsilon^+$, represents the temperature dependent isotopic effect of a change in phase from liquid to vapour on $\Delta_e$ as follows, where $T_l$ is leaf temperature in Kelvin (Bottinga and Craig 1969):

$$\varepsilon^+(‰) = 2.644 - 3.206\left(\frac{10^3}{T_l}\right) + 1.534\left(\frac{10^6}{T_l^2}\right), \qquad (4)$$

$\varepsilon_k$ represents the isotopic effect of diffusion on $H_2{}^{18}O$ through the stomatal ($g_s$) and boundary ($g_b$) layers (Eqn. 5; Farquhar et al. 1989) incorporating the discrimination values determined by Merlivat (1978):

$$\varepsilon_k = \frac{28g_s^{-1} + 18.7g_b^{-1}}{g_s^{-1} + g_b^{-1}}. \qquad (5)$$

The steady-state formulation (Eqn. 3, but expressed relative to the Vienna Standard Mean Ocean Water standard VSMOW) can be adapted for both steady-state and non-steady-state conditions following Harwood et al. (1998):

$$\delta_e = \delta_{trans} + \varepsilon^+ + \varepsilon_k + (\,(\delta_v - \varepsilon_k - \delta_{trans}) \times {}^{e_a}/_{e_i}\,). \qquad (6)$$

In Eqn. 6, $\delta_{trans}$ is the isotopic composition of transpired water and $\delta_v$ is the vapour in the leaf chamber, both relative to VSMOW. In this study, the incoming air was dry, so $\delta_v$ is entirely derived from $\delta_{trans}$.

The Craig-Gordon model was modified (Farquhar and Lloyd 1993) to account for the observed discrepancy between measured leaf water enrichment ($\Delta_L$) and modelled $\Delta_e$:

$$\Delta_L = \frac{\Delta_e(1-e^{-\wp})}{\wp}, \qquad (7)$$

where $\wp$ is the Péclet number and describes the enrichment of water flowing towards the sites of evaporation from the backwards diffusion of $H_2{}^{18}O$:

$$\wp = \frac{EL}{CD}, \qquad (8)$$

where $E$ is transpiration rate (mol $m^{-2}$ $s^{-1}$), $L$ is the effective path length (m), $C$ is the molar density of water (mol $m^{-3}$) and $D$ ($m^2$ $s^{-1}$) is the diffusivity of $H_2{}^{18}O$ in water, which varies with leaf temperature (Cuntz et al. 2007):

$$D = 97 \times 10^{-9} \times exp^{\left(\frac{-577}{((T_l+273.16)-145)}\right)}. \qquad (9)$$

The Péclet effect predicts a positive relationship between $E$ and $1-\Delta_L/\Delta_e$. For each replicate, $L$ was fitted by minimising the difference between the measured $\Delta_L$ and modelled $\Delta_{LS}$ using Eqn. 7. For comparison with the two-pool model, these individual values were averaged and the mean value then used to estimate bulk leaf water.

The Two-pool model

The simplest form of the discrete-pool model, the two-pool model assumes that bulk leaf water is the combination of two pools of water, one in the veins that is not subjected to evaporative enrichment and is therefore isotopically similar to source water and one in the lamina tissue that is influenced by evaporative enrichment (Leaney et al. 1985). The predicted oxygen isotope composition of leaf water assuming two pools ($\Delta_{L\_t}$) is described as:

$$\Delta_{L\_t} = (1 - \phi)\Delta_e, \qquad (12)$$

where $\phi$ is the fraction of unenriched water in the veins. $\phi$ was assumed to be equal to $1-\Delta_L/\Delta_e$ (Song et al. 2015), but note that we use $\phi$ when discussing the two pool model in order to avoid potential confusion. For comparison with the Péclet effect model, the two-pool model was run using the average value of $\phi$ for each species.

Statistical Analysis

Data was graphed using Origin (Version 6.1; OriginLab Corp, Northampton, Massachusetts, USA). Significant linear relationships were defined by a *p*-value of less than 0.05. A two-sample *t*-test was performed in Genstat (Version 16, VSN International Ltd, www.vsni.co.uk) to assess the difference between isotopic steady state and non-steady-state estimates of $1 - \Delta_L/\Delta_e$ calculated for *H. annuus*. Predictions from the two-pool and Péclet effect models were plotted against measured bulk leaf water and the linear relationship was analysed using a Student's *t*-test. The null hypothesis was that the slope and intercept did not differ from a 1:1 line (i.e. the slope was not different from 1, and the intercept not different from zero) as described in Bailey (1981), where *t* = (1-slope[or intercept])/standard error of the slope[or intercept].

## RESULTS

For the 21 species measured in this study, leaf anatomical properties were assessed visually using either light microscopy or published cross-sections, to place each species into one of the three hydraulic designs suggested by Zwieniecki et al. (2007). The results are presented in Table 1, with the average values for the Craig-Gordon estimate, the bulk leaf water and effective path length shown in Supp. Table 1. In addition, we have included another 11 species from previously published studies for which the relationship between $E$ and $1-\Delta_L/\Delta_e$ could be determined and for which the anatomical properties were available in the literature. Of our 21 species, six were determined to be closest anatomically to Design 1 (usually no bundle sheath extension and unstructured mesophyll), eight were assigned to Design 2 (usually a bundle sheath extension and mesophyll structured into spongy and palisade mesophyll layers) and seven to Design 3 (palisade and spongy mesophyll cells are indistinct). Note that while Zwieniecki et al. (2007) classified adult *E. globulus* leaves as Design 3, we have classified the juvenile *E, globulus* as Design 2 due to the presence of bundle sheath extension cells and a mesophyll structured into spongy and palisade layers. Based on the hydraulic designs, we predicted a whole leaf Péclet effect would be detected in Design 2 leaves only, with Design 1 and 3 leaves displaying no significant positive relationship between $E$ and $\Delta_L/\Delta_e$.

The relationships between transpiration rate ($E$) and $1-\Delta_L/\Delta_e$ in bulk leaf water (i.e. mid vein and lamina tissue combined) are shown for 18 species in Fig. 1. For these measurements the whole leaf, or a section of the lamina that remained intact (i.e. the major vein was not removed) was used, revealing that all 18 have a relationship between $E$ and $1-\Delta_L/\Delta_e$ that is consistent with their

assigned Design (Fig. 1). The species *Acer x freemanii*, *E. camaldulensis*, *E. globulus*, *E. grandis*, *E. polybractea*, *G. hirsutum* and *V. vinifera* showed a significant positive relationship between $E$ and $1-\Delta_L/\Delta_e$ ($p < 0.05$; Fig. 1E to 1L). The remaining species showed either no significant correlation between $E$ and $1-\Delta_L/\Delta_e$ ($p > 0.05$; Fig. 1; *E. parramattensis*, *E. amplifolia*, *E. occidentalis*, *E. stellulata*, *G. biloba*, *G. max*, *H. annuus*, *T. aestivum*, and ambient light and $CO_2$ grown *V. faba*), or in the case of *V. faba, C. arietinum and E. botryoides* a significantly negative relationship between $E$ and $1 - \Delta_L/\Delta_e$. *P. vulgaris*, while being assigned to Design 2, was marginally non-significant ($p = 0.06$; Fig. 1K).

Different growth and measurement conditions, and techniques for analysing leaf water isotope composition, were included in the study. For *V. faba*, differences in growth conditions were compared (Supplementary Fig. S1), in *H. annuus* the necessity to reach isotopic steady state was assessed (Fig. 1R), and three species (*H. annuus*, *E. parramattensis* and *E. grandis*) were used to assess the effects of measurement irradiance on the relationship between $E$ and $1 - \Delta_L/\Delta_e$ (Figure 2). For *V. faba*, no significant differences were found between genotypes, so all genotypes were pooled for subsequent analysis. A significant positive relationship was found for leaves of plants grown in low light, ambient $CO_2$ conditions ($p = 0.004$; Supp. Fig. 1D), while a negative relationship was found for leaves grown at low light and high $CO_2$ conditions ($p < 0.0001$; Supp. Fig. 1B) and no significant relationship was found for leaves grown at high light and either high or ambient $CO_2$ concentration (Supp. Fig. 1A and C). For *H. annuus*, samples taken at isotopic steady state had higher $1 - \Delta_L/\Delta_e$ values than those for which steady state was not achieved, but in both situations there were non-significant relationships between transpiration rate and $1-\Delta_L/\Delta_e$. As shown in Fig. 2, there were no significant differences in the relationship between $E$ and $1-\Delta_L/\Delta_e$ for low (200 μmol $m^{-2}$ $s^{-1}$) and high (1200 μmol $m^{-2}$ $s^{-1}$) irradiance measurements for any

315 of the three species assessed. We conclude that data presented in Fig. 1 do not include artefacts
316 due to changes in irradiance. A significant positive relationship between $E$ and $1-\Delta_L/\Delta_e$ was
317 observed for *H. annuus* when measurements were made at 200 and 1200 mmol $m^{-2}$ $s^{-1}$ irradiance
318 (Fig. 2A), which differs from the non-significant relationships between $E$ and $1-\Delta_L/\Delta_e$ for this
319 species in Fig. 1R. However, it should be noted that the relationship in Fig 2A is strongly driven
320 by a single point at low $E$.

321 The appropriateness of using a Péclet model or two-pool model for estimating leaf water isotopic
322 enrichment was assessed. For direct comparison, the species average $L$ (for the Péclet model) and
323 $\phi$ (for the two-pool model) were applied to all replicates for each species and then the predicted
324 leaf water enrichment was tested for deviation from a 1:1 relationship with the measured bulk
325 leaf water values. A non-significant $p$-value indicated that the regression slope and intercept
326 were similar to a regression assuming the model gave exact predictions of measured bulk leaf
327 water. Species that were categorised as either Design 1 or Design 3 were generally better
328 modelled using a two-pool model and those in Design 2 were generally better modelled using the
329 Péclet effect model (Supp. Table 2). For *E. amplifolia*, *E. botryoides*, *G. hirsutum*, *G. max*, *C.*
330 *arientinum* and *V. faba* (except ambient $CO_2$ and low irradiance) neither model proved able to
331 predict bulk leaf water particularly well (Supp. Table 2).

332 Eight species, including *C. sasanqua* and *W. nobilis*, were also measured and the major vein and
333 lamina sampled and analysed separately for stable isotope composition. A composite value for
334 the whole leaf was estimated by combining water contents and isotope compositions. Fig. 3
335 shows the relationships between $E$ and $1-\Delta_L/\Delta_e$, with the species separated into hydraulic design
336 (again determined based on anatomy). There was a significant positive relationship between $E$
337 and $1-\Delta_L/\Delta_e$ for *C. sasanqua* lamina ($p = 0.02$; $R^2 = 0.49$) primary vein ($p = 0.0003$, $R^2 = 0.82$)

and the composite estimate ($p = 0.003$, $R^2 = 0.69$; Fig. 2A). However, half of the *C. sasanqua* lamina samples had negative values of $1-\Delta_L/\Delta_e$ (i.e. $\Delta^{18}O_L > \Delta^{18}O_e$), despite these measurements being made at isotopic steady state (or very close to). The results for *W. nobilis* were similar: the lamina, vein and composite *f* were all significantly correlated with *E* ($p = 0.02$, $R^2 = 0.35$; $p < 0.001$, $R^2 = 0.75$ and $p < 0.001$, $R^2 = 0.68$ respectively) despite more than half of the lamina $1-\Delta_L/\Delta_e$ being negative (Fig. 3B). For *Acer x freemanii* and the *Eucalyptus* species, as many as half of the lamina samples had a negative value of $1-\Delta_L/\Delta_e$. *E. occidentalis* and *E. polybractea* showed no significant relationship between *E* and $1-\Delta_L/\Delta_e$, calculated either from lamina, primary vein or the composite of both ($p > 0.05$; Fig. 3G and F). There was a significant correlation between *E* and primary vein $1-\Delta_L/\Delta_e$ for *E. stellulata* ($p = 0.0002$; $R^2 = 0.66$; Fig. 3H) but not with $1-\Delta_L/\Delta_e$ calculated from the lamina or composite of both. Both *E. camaldulensis* and *E. grandis* showed significant correlations between *E* and $1-\Delta_L/\Delta_e$ calculated from all three measurements (primary vein, lamina and composite, $p < 0.001$; Fig. 2D and E). For *Acer x freemanii*, only $1-\Delta_L/\Delta_e$ calculated from the primary vein measurements showed a significant relationship with *E* ($p < 0.0001$, $R^2 = 0.71$; Fig. 3C).

## DISCUSSION

### *Is the Craig-Gordon model sufficient to predict leaf water enrichment?*

The motivation for development of both the two-pool and Péclet models of leaf water enrichment were observations that the Craig-Gordon model over-estimated enrichment at isotopic steady state. Early studies revealing a positive relationship between *E* and $1-\Delta_L/\Delta_e$, either directly

(Flanagan et al. 1994), or indirectly (Barbour et al. 2000; Barbour et al. 2004), have used this as evidence for the relevance of using the Péclet model to predict whole leaf enrichment. However, more a recent study with *G. hirsutum* (Song et al. 2015) found a slightly positive but non-significant relationship between $E$ and $1-\Delta_L/\Delta_e$, suggesting that the two-pool model may be more appropriate. The core test of the relevance of either the two-pool or the Péclet model for leaf water is that bulk leaf water is less enriched than that predicted by the Craig-Gordon model when the leaf is at isotopic steady state. Among the species studied here, we found that no more than a third of the values of $1-\Delta_L/\Delta_e$ were negative in 19 of the 21 species. $\Delta_L$ was always less that $\Delta_{es}$ in *G. biloba*, *T. aestivum*, *E. globulus*, *E. parramettensis*, *G. hirsutum*, *P. vulgaris*, *V. vinifera*, *G. max* and *H. annuus*, suggesting that the Craig-Gordon alone model is insufficient for predicting $\Delta_L$. Measurements of lamina isotope composition in *C. sasanqua* and *W. nobilis* indicate that $\Delta_L > \Delta_e$ in more than half the samples for these two species, but there were significant positive relationships between $E$ and $1-\Delta_L/\Delta_e$ for the mid-veins, lamina tissue and the calculated composite bulk leaf water. Both these species were classified as Design 1 and both have very low transpiration rates (< 1.5 mmol $m^{-2}$ $s^{-1}$), and so may not have been at isotopic steady state despite remaining in the leaf chamber for up to 7 hours. For these species, and potentially other species with low rates of $E$, a more complicated non-steady state expression may be required for both the two-pool and the Péclet model; a model that includes pools of hydraulically disconnected water with very low turnover times. The models tested here are the simplest versions, more complicated versions of the Péclet model being found in Gan et al. (2003), Ogée et al. (2007) and Cuntz et al. (2007).

We also observed negative relationships between $E$ and $1-\Delta_L/\Delta_e$ for *C. arientinum*, *E. botryoides* and *V. faba* (for plants grown and measured at high $CO_2$ concentrations and both high and low

383 light levels). We currently lack an explanation for these unexpected observations, but clearly the
384 Péclet effect is not relevant for these species and growth conditions. The two-pool model also
385 needs to be modified to account for negative relationships; a higher value of $\phi$ when transpiration
386 rates are low.

387 We conclude that the Craig-Gordon model is insufficient to explain observed variation in $\Delta_L$, and
388 that either the two-pool model (for leaf hydraulic designs 1 and 3) or the Péclet effect model (for
389 hydraulic design 2) are required to predict $\Delta_L$. Figure 4 shows that the Craig-Gordon model
390 over-estimates $\Delta_L$ by 4.8‰ on average, and by as much as 12.5‰. In contrast, using an
391 appropriate, hydraulically-informed, model results in an average difference between measured
392 and modelled values of just 0.01‰.
393

394 *Considering hydraulic design and leaf water isotopes*

395 Using rehydration kinetic measurements, Zwieniecki et al. (2007) proposed three hydraulic
396 designs for leaves with differing pathways for water movement and levels of mesophyll water
397 connectedness. These hydraulic designs imply differences in the proportion of the transpiration
398 stream moving within the apoplastic and symplastic pathways. We have previously suggested
399 that the relative importance of apoplastic and symplastic pathways is relevant to leaf water
400 isotopes (Barbour and Farquhar 2003). Apoplastic water movement is assumed to be dominated
401 by bulk flow (Strugger 1943) and as the Péclet effect describes the ratio of advection to
402 convection in mass flow, it is likely that apoplastic pathways will allow isotopic gradients to
403 form. In contrast, symplastic water transport through plasmodesmata and transcellular transport
404 across cellular membranes may not allow isotopic gradients to form. This is because aquaporins

405 and the pores of plasmodesmata are thought to be too small to support bulk flow (Schaffner
406 1998; Fricke 2000). The pore of an aquaporin is thought to be only large enough for a single
407 water molecule to move through (Schaffner 1998), and it is unlikely that isotopic gradients could
408 be formed for molecules moving in single file. If a high proportion of the transpiration stream
409 moves from the xylem to the sites of evaporation through aquaporins, isotopic gradients may not
410 form in the cytoplasm or, as we suggested, may be poorly described by Péclet effect theory.
411 However, if any water molecules move counter to the net flow, isotopic gradients may form
412 (Barbour and Farquhar 2003). Additionally, it is unclear what role, if any, the vacuole may have
413 in the development of isotopic heterogeneity. As the vacuole can contain a large proportion of
414 cellular water, how this pool of water is involved in the transpiration stream may have a
415 significant effect on isotopic composition at the whole leaf level.

416 Relating pathways of water transport to water isotopes, we suggest that liquid water transport in
417 the apoplast would allow the development of Péclet-type gradients in enrichment if the ratio
418 between water velocity times characteristic length and $H_2{}^{18}O$ diffusivity in water were of the
419 appropriate order of magnitude (see Eqn 13). We assume that water transport through
420 aquaporins would not allow isotopic gradients to form across membranes (Barbour and Farquhar
421 2003) and that transport in the vapour phase will not allow a gradient in enrichment to develop in
422 the liquid phase. Therefore, the ability to detect a Péclet effect at the whole leaf level will
423 depend on the contribution of apoplastic and symplastic pathways to water movement.

424 For a given transpiration rate, the velocity at which water moves through specific pathways
425 within leaves is related to differences in hydraulic resistance and the cross sectional area
426 perpendicular to direction of flow (Barbour and Farquhar 2003). The Péclet effect is determined
427 by $\wp$, the product of the velocity of water movement ($v$, m $s^{-1}$) and the distance from the

evaporation sites ($l$, m) in ratio to the diffusivity of $H_2{}^{18}O$ in water ($D$, $m^2\ s^{-1}$, variable with temperature) (Barbour and Farquhar 2003):

$$\wp = \frac{vl}{D} \quad . \quad (13)$$

A significant Péclet effect occurs when there is a high velocity, a long diffusional distance or a combination of both. Presence of a Péclet effect implies a low resistance pathway from veins to evaporation sites that has a small cross-sectional area perpendicular to the direction of flow. These characteristics are consistent with water transport in the apoplast (Rockwell, Holbrook and Stroock, 2014; Buckley 2015). On the contrary, low velocity would suggest a high resistance and/or a large cross sectional area perpendicular to the direction of flow, and in these instances isotopic gradients may not form (i.e. no Péclet effect).

The detection of a whole leaf Péclet effect is likely to be related to how variation in mesophyll hydraulic resistance and cross sectional area of liquid transport pathways affect the velocity of water movement, and to some extent, how the distance to the evaporation sites varies with leaf anatomy. Stomatal density and the ratio of densities on abaxial and adaxial leaf surfaces is likely to influence this distance and may be relevant for the development of Péclet gradients within leaves. We note that Larcher et al. (2014) observed a positive relationship between stomatal density and $\Delta_L/\Delta_e$, but point out that this study assumed that a Péclet effect was present in all genotypes and species which we have shown here may not be the case.

In Design 2 leaves, water primarily moves from the xylem to the epidermis through bundle sheath extensions then along the epidermal cells towards the nearest stoma because there is a high degree of hydraulic resistance between the xylem and the mesophyll. In this situation, liquid water transport through the lamina is likely dominated by apoplastic flow (e.g. Rockwell,

Holbrook and Stroock 2014; Buckley 2015) with associated isotope gradients. A possible explanation for the high mesophyll resistance in Design 2 leaves is a low expression of aquaporins in the plasma membranes of mesophyll cells. These features combine to produce high velocity for liquid transport within the low resistance and small area pathways in the apoplast of the xylem, bundle sheath extension and epidermal cells. Gradients in enrichment are likely within the apoplast of bundle sheath extension and epidermal cells in Design 2 leaves. These gradients could then propagate from the bundle sheath extension cells through the adjacent mesophyll cells via establishment of local isotopic equilibria. Note that this local equilibrium does not rely on isotope gradients forming through membranes and their associated aquaporins. Rather, over time water in the hydraulically-disconnected mesophyll cells would exchange and isotopically equilibrate with water in the adjacent bundle sheath extension and epidermal cells.

By comparison, species with leaves fitting in Design 3 classification presumably have high expression of aquaporins, allowing water to rapidly traverse the mesophyll, while also being transported through the bundle sheath extensions around the xylem. In these leaves, the high expression of aquaporins may preclude the development of gradients in enrichment between the sites of evaporation and the veins, so water in the mesophyll will have an isotopic composition similar to the evaporative sites within the leaf and hence no Péclet effect. In leaves with limited hydraulic connections between the veins and either the epidermis or the mesophyll (Design 1), the low velocity water transport through high resistance pathways would also preclude formation of isotope gradients within the mesophyll.

*Can hydraulic design explain differences between leaves in the relevance of the Péclet effect?*

Combining the use of variation in $H_2{}^{18}O$ with leaf hydraulics to understand water movement through leaves seems obvious and yet these two techniques are rarely measured simultaneously (but see Kahmen et al. 2009; Ferrio et al. 2012; Loucos et al. 2015). Here we show a novel link between leaf hydraulic designs constrained by different leaf anatomy (Zwieniecki et al. 2007) and the patterns of isotopic enrichment at the whole leaf level, suggesting that we are closer to reconciling the contrasting results across the literature. For instance, by identifying that only species Design 2 leaf anatomy will have a clear Péclet effect at the whole leaf level we offer an explanation for why some species have exhibited Péclet effects and others not.

Focusing on Design 2 leaves, the anatomical features of these species may allow the formation of a Péclet effect in the bundle sheath extensions and apoplastic pathway. As shown in Fig. 1, species placed into Design 2 were found to have a significant relationship between $E$ and $1-\Delta_L/\Delta_e$ (except *P. vulgaris* which was marginally non-significant Fig. 1K, and *E. polybractea* when main veins and lamina tissue were sampled separately Fig. 3F). In support of these results, our analysis of the best fit model for the data of each species reveal that the Péclet model is a better fit for species with Design 2 leaves than the two-pool (Supp. Table 2). This contrasts to data for leaves from Design 1 or Design 3, in which generally the two-pool model provided equal or better fit than the Péclet effect (Supp. Table 2). Indeed our isotope results show that Design 1 and 3 leaves, in which a Péclet effect is not expected to form across the whole leaf, have no relationship between $E$ and $1-\Delta_L/\Delta_e$ (Fig. 1).

The lack of a Péclet effect at the whole leaf level does not necessarily exclude a localised Péclet effect occurring in the veins and associated tissue, as suggested by the significant positive

494 relationship between $E$ and $1-\Delta_L/\Delta_e$ for primary vein samples of *G. hirsutum* (Holloway-Phillips
495 et al. 2016). The results presented here support the notion that the positive relationship between
496 $E$ and $1-\Delta_L/\Delta_e$ occurs strongly in the primary veins (6 of 8 species in Fig. 3, $p < 0.05$) and is
497 therefore likely to occur in lower order veins. However, even when there was a significant
498 relationship between $E$ and $1-\Delta_L/\Delta_e$ in leaf sections containing a primary vein, this was not
499 enough to drive a significant positive relationship between $E$ and $1-\Delta_L/\Delta_e$ in the composite leaf
500 estimate (e.g. *Acer* and *E. polybractea*). For the *Eucalyptus* species where there was a significant
501 leaf composite $E$ and $1-\Delta_L/\Delta_e$ relationship, there was also a significant relationship between $E$
502 and $1-\Delta_L/\Delta_e$ in the lamina (which contained minor veins; Fig. 3). Design 1 leaves are expected to
503 have low velocity of liquid transport due to either low transpiration rates (e.g. gymnosperm
504 species and *C. sasanqua*) or an absence of low resistance pathways (i.e. no bundle sheath
505 extensions) meaning that water transport from the veins to the stomata likely occurs through the
506 entire mesophyll with large associated cross sectional area. In both cases, we suggest this will
507 result in no detectable whole leaf Péclet effect. For Design 3 leaves, water movement through the
508 well-connected mesophyll will greatly increase the cross-sectional area for flow, resulting in a
509 slower velocity across the whole leaf and, combined with a dominance of aquaporin transport
510 that doesn't allow gradients to develop, no Péclet effect is detectable at the whole leaf level.
511 Combining hydraulic design and isotope theory, our results suggest that the main pathway in
512 which a Péclet effect may form is located in the apoplastic pathways, including through the
513 bundle sheath extensions. However, we stress that the link between isotopic patterns and leaf
514 hydraulics has yet to be tested in a wide range of environmental conditions and we have relied on
515 leaf anatomy to assess hydraulic design. A more rigorous test of the relationship would include
516 measurements of leaf rehydration kinetics to determine hydraulic design. Finally, stomatal

density (Larcher et al. 2014) and the presence of stomata on both leaf surfaces could influence the strength of the observed Péclet effect for Design 2 leaves; this would be an interesting area for future studies.

*Conclusions*

The most appropriate model for predicting whole leaf lamina isotopic enrichment has remained elusive. Evidence in support of the two most commonly used models, the Péclet model and the two-pool model, has been found in the literature but until now there has been no way to determine when a particular model is suitable. We demonstrate that the Péclet effect is relevant at the whole leaf level for less than 50% of sampled species. We relate these findings to the leaf hydraulic designs proposed by Zwieniecki et al. (2007), in which only species from Design 2 exhibit a detectable Péclet effect at the whole leaf level. It was generally found that for species with no correlation between $E$ and $1-\Delta_L/\Delta_e$, the two-pool model was equal to or better than the simplest version of the Péclet model at predicting bulk leaf water enrichment.

**Conflict of interest statement:** The authors have no conflicts of interest to declare.

## REFERENCES

Aasamaa K., Niinemets Ü., & Sõber A. (2005) Leaf hydraulic conductance in relation to anatomical and functional traits during *Populus tremula* leaf ontogeny. *Tree Physiology* **25**, 1409-1418.

538 Bailey N.T.J. (1981) *Statistical Methods in Biology*. 2nd Edn. John Wiley and Sons: New York,
539 USA.

540 Barbour M.M. & Farquhar G.D. (2003) Do pathways of water movement and leaf anatomical
541 dimensions allow development of gradients in $H_2{}^{18}O$ between veins and the sites of
542 evaporation within leaves? *Plant Cell & Environment* **27**, 107-121.

543 Barbour M.M., Roden J.S., Farquhar G.D. & Ehleringer J.R. (2004) Expressing leaf water and
544 cellulose oxygen isotope ratios as enrichment above source water reveals evidence of a
545 Péclet effect. *Oecologia* **138**, 426-435.

546 Barbour M.M., Schurr U., Henry B.K., Wong S.C. & Farquhar G.D. (2000) Variation in the
547 oxygen isotope ratio of phloem sap sucrose from castor bean. Evidence in support of the
548 Péclet Effect. *Plant Physiology* **123**, 671-679.

549 Bender M., Sowers T. & Labeyrie L. (1994) The Dole effect and its variations during the last
550 130,000 years as measured in the Vostok ice core. *Global Biogeochemical Cycles* **8**, 363-
551 376.

552 Bostrack J.M & Sparrow A.H. (1969) Effects of chronic gamma irradiation on the anatomy of
553 vegetative tissues of *Pinus rigida* Mill. *Radiation Botany* **9**, 367-374.

554 Bottinga Y. & Craig H. (1969) Oxygen isotope fractionation between $CO_2$ and water, and the
555 isotopic composition of marine atmospheric $CO_2$. *Earth and Planetary Science Letters* **5**,
556 285-295.

557 Buckley T.N. (2015) The contributions of apoplastic, symplastic and gas phase pathways for
558 water transport outside the bundle sheath in leaves. *Plant, Cell & Environment* **38**, 7-22.

559 Buckley T.N., John G.P., Scoffoni C. & Sack L. (2017) The sites of evaporation within leaves.
560 *Plant Physiology* **173**, 1763-1782.

561 Burrows G.E. & Bullock S. (1999) Leaf anatomy of wollemi pine (*Wollemia nobilis*,
562 Araucariaceae). *Australian Journal of Botany* **47**, 795-806.

563 Cernusak L.A., Barbour M.M., Arndt S.K., Cheesman A.W., English N.B., Feild T.S., Helliker
564 B.R., Holloway-Phillips M.M., Holtum J.A.M., Kahmen A., McInerney F.A.,
565 Munksgaard N.C., Simonin K.A., Song X., Stuart-Williams H., West J.B. & Farquhar
566 G.D. (2016) Stable isotopes in leaf water of terrestrial plants. *Plant, Cell & Environment*
567 **39**, 1087-1102.

568 Ciais P., Tans P.P., Denning A.S., Francey R.J., Trolier M., Meijer H.A.J., White J.W.C., Berry
569 J.A., Randall D.A., Collatz G.J., Sellers P.J., Monfray P. & Heimann M. (1997) A
570 three-dimensional synthesis study of $\delta^{18}O$ in atmospheric $CO_2$. 2. Simulations with the
571 Tm2 transport model. *Journal of Geophysical Research-Atmospheres* **102**, 5873-5883.

572 Craig H. & Gordon L.I. (1965) Deuterium and oxygen-18 variations in the ocean and the marine
573 atmosphere. In E Tongiorgi, ed, *Proceedings of a conference on stable isotopes in*
574 *oceanographic studies and paleotemperatures*. Laboratory of Geology and Nuclear
575 Science, Pisa, pp 9-130.

576 Cuntz M., Ogée J., Farquhar G.D., Peylin P., Cernusak L.A. (2007) Modelling advection and
577 diffusion of water isotopologues in leaves. *Plant, Cell & Environment* **30**, 892-909.

578 Dole M., Lane G.A., Rudd D.P. & Zaukelies D.A. (1954) Isotopic composition of atmospheric
579 oxygen and nitrogen. *Geochimica et Cosmochimica Acta* **6**, 65-78.

Dongmann G., Nurnberg H.E., Forstel H. & Wagener K. (1974) On the enrichment of $H_2{}^{18}O$ in the leaves of transpiring plants. *Radiation and Environmental Biophysics* **11**, 41-52.

Farquhar G.D., Hubick K.T., Condon A.G. & Richards R.A. (1989) Carbon isotope fractionation and plant water-use efficiency. In *Stable Isotopes in Ecological Research*. PW Rundel, JR Ehleringer and KA Nagy (eds). Springer Verlag, New York, pp 21-40.

Farquhar G.D. & Lloyd J. (1993) Carbon and oxygen isotope effects in the exchange of carbon dioxide between terrestrial plants and the atmosphere. In JR Ehleringer, AE Hall, GD Farquhar, eds, *Stable isotopes and plant carbon-water relations*. Academic Press, San Diego, pp 47-70.

Ferrio J.P., Cuntz M., Offermann C., Siegwolf R., Saurer M. & Gessler A (2009) Effect of water availability on leaf water isotopic enrichment in beech seedlings shows limitation of current fractionation models. *Plant, Cell & Environment* **32**, 1285-1296.

Ferrio J.P., Pou A., Florez-Sarasa I., Gessler A., Kodama N., Flexas J. & Ribas-Carbó M. (2012) The Péclet effect on leaf water enrichment correlates with leaf hydraulic conductance and mesophyll conductance for $CO_2$. *Plant, Cell & Environment* **35**, 611-625.

Fisher D.G. & Evert R.F. (1982) Studies on the leaf of *Amaranthus retroflexus* (Amaranthaceae): Morphology and Anatomy. *American Journal of Botany* **69**, 1133-1147.

Flanagan L.B., Comstock J.P. & Ehleringer J.R. (1991) Comparison of modelled and observed environmental influences on the stable oxygen and hydrogen isotope composition of leaf water in *Phaseolus vulgaris* L. *Plant Physiology* **96**, 588-596.

Flanagan L.B., Phillips S.L., Ehleringer J.R., Lloyd J. & Farquhar G.D. (1994) Effect of changes in leaf water oxygen isotopic composition on discrimination against $C^{18}O^{16}O$ during photosynthetic gas-exchange. *Australian Journal of Plant Physiology* **21**, 221-234.

Fricke W. (2000) Water movement between epidermal cells of barley leaves – a symplastic connection? *Plant, Cell & Environment* **23**, 991-997.

Gan K.S., Wong C.S., Yong J.W.H. & Farquhar G.D. (2003) Evaluation of models of leaf water $^{18}O$ enrichment using measurements of spatial patterns of vein xylem water, leaf water and dry matter in maize leaves. *Plant, Cell and Environment* **14**, 1479-1495.

Harwood K.G., Gillon J.S., Griffiths H. & Broadmeadow M.S.J. (1998) Diurnal variation of $\Delta^{13}CO_2$, $\Delta C^{18}O^{16}O$ and evaporative site enrichment of $\delta H_2{}^{18}O$ in *Piper aduncum* under field conditions in Trinidad. *Plant, Cell & Environment* **21**, 269-283.

Helliker B.R. & Richter S.L. (2008) Subtropical to boreal convergence of tree-leaf temperatures. *Nature* **454**, 551-514.

Holloway-Phillips M.M., Cernusak L.A., Barbour M.M., Song X., Cheesman A., Munksgaard N., Stuart-Williams H. & Farquhar G.D. (2016) Leaf vein fraction influences the Péclet effect and $^{18}O$ enrichment in leaf water. *Plant, Cell & Environment* **39**, 2414-2427.

Jahan E. (2016) Genotypic, environmental and leaf anatomical effects on mesophyll conductance in wheat (*Triticum aestivum* L.). PhD thesis. University of Sydney, Australia.

James S.A., Smith W.K. & Vogelmann T.C. (1999) Ontogenetic differences in mesophyll structure and chlorophyll distribution in *Eucalyptus globulus* ssp. *globulus* (Myrtaceae). *American Journal of Botany* **82**, 198-207.

621 John G.P., Scoffoni C. & Sack L. (2013) Allometry of cells and tissues within leaves. *American*
622 *Journal of Botany* **100**, 1936-1948.

623 Junior J.L., Malavolta E., Nogueira N.dL., Moraes M.F., Reis A.R., Rossi M.L. & Cabral C.P.
624 (2009) Changes in anatomy and root cell ultrastructure of soybean genotypes under
625 manganese stress. *Revista Brasileira de Ciencia do Solo* **33**, 395-403.

626 Kahmen A., Simonin K., Tu K., Goldsmith G.R. & Dawson T.E. (2009) The influence of species
627 and growing conditions on the 18-O enrichment of leaf water and its impact on 'effective
628 path length'. *New Phytologist* **184**, 619-630.

629 Karki S., Rizal G. & Quick W.P. (2013) Improvement of photosynthesis in rice (*Oryza sativa* L.)
630 by inserting the C4 pathway. *Rice* **6**, 28.

631 Larcher L., Hara-Nishimura I. & Sternberg L. (2014) Effects of stomatal density and leaf water
632 content on the $^{18}O$ enrichment of leaf water. *New Phytologist* **206**, 141-151.

633 Leaney F.W., Osmond C.B., Allison G.B. & Ziegler H. (1985) Hydrogen-isotope composition of
634 leaf water in $C_3$ and $C_4$ plants: its relationship to the hydrogen-isotope composition of dry
635 matter. *Planta* **164**, 215-220.

636 Libby L.M., Pandolfi L.J., Payton P.H., Marshall J.III, Becker B. & Giertz-Sienbenlist V. (1976)
637 Isotopic tree thermometers. *Nature* **261**, 284-288.

638 Loucos K.E., Simonin K.A., Song X. & Barbour M.M. (2015) Observed relationships between
639 leaf $H_2{}^{18}O$ Péclet effective length and leaf hydraulic conductance reflect assumptions in
640 Craig-Gordon model calculations. *Tree Physiology* **35**, 16-26.

641 Merlivat L. (1978) Molecular diffusivities of $H_2{}^{16}O$, $HD^{16}O$ and $H_2{}^{18}O$ in gases. *Journal of*
642 *Chemical Physics* **69**, 2864-2871.

643 Morison J.I.L., Lawson T. & Cornic G. (2007) Lateral $CO_2$ diffusion inside dicotyledonous
644 leaves can be substantial: Quantification in different light intensities. *Plant Physiology*
645 **145**, 680-690.

646 Ogée J., Cuntz M., Peylin P. & Bariac T. (2007) Non-steady-state, non-uniform transpiration rate
647 and leaf anatomy effects on the progressive stable isotope enrichment of leaf water along
648 monocot leaves. *Plant, Cell and Environment* **30**, 367-387.

649 Pengelly J.J.L., Sirault X.R.R., Tazoe Y., Evans J.R., Furbank R.T. & von Caemmerer S. (2010)
650 Growth of the $C_4$ dicot *Flaveria bidentis*: photosynthetic acclimation to low light through
651 shifts in leaf anatomy and biochemistry. *Journal of Experimental Botany* **61**, 4109-4122.

652 Pérez Chaca M.V., Vigliocco A., Reinoso H., Molina A., Abdala G., Zirulnik F. & Pedranzani H.
653 (2014) Effects of cadmium stress on growth, anatomy and hormone contents in *Glycine*
654 *max* (L.) Merr. *Acta Physiologiae Plantarum* **36**, 2815-2826.

655 Ripullone F., Matsuo N., Stuart-Williams H., Wong S.C., Borghetti M., Tani M. & Farquhar
656 G.D. (2008) Environmental effects on oxygen isotope enrichment of leaf water in cotton
657 leaves. *Plant Physiology* **146**, 729-736.

658 Rockwell F.E., Holbrook N.M. & Stroock A.D. (2014) The competition between liquid and
659 vapour transport in transpiring leaves. *Plant Physiology* **164**, 1741-1758.

660 Roden J.S., Canny M.J., Huang C.X. & Ball M.C. (2009) Frost tolerance and ice formation in
661 *Pinus radiata* needles: ice management by the endodermis and transfusion tissues.
662 *Functional Plant Biology* **36**, 180-189

663 Roden J., Kahmen A., Buchmann N. & Siegwolf R. (2015) The enigma of effective path length
664 for $^{18}O$ enrichment in leaf water of conifers. *Plant, Cell & Environment* **38**, 2551-2565.

665 Santos L.D.T., Thadeo M., Iarema L., Alves Meira R.M.S. & Ferreira F.A. (2008) Foliar
666 anatomy and histochemistry in seven species of *Eucalyptus*. *Revista Arvore* **32**, 769-779.

667 Schäffner A.R. (1998) Aquaporin function, structure and expression: are there more surprises to
668 surface in water relations? *Planta* **204**, 131-139.

669 Sefton C.A., Montagu K.D., Atwell B.J. & Conroy J.P. (2002) Anatomical variation in juvenile
670 eucalypt leaves accounts for differences in specific leaf area and $CO_2$ assimilation rates.
671 *Australian Journal of Botany* **50**, 301-310.

672 Simonin K.A., Roddy A.B.., Link P, Apodaca R., Tu K.P., Hu J., Dawson T.E. & Barbour MM
673 (2013) The isotopic composition of transpiration and rates of change in leaf water
674 isotopologue storage in response to environmental variables. *Plant, Cell & Environment*
675 **36**, 2190-2206.

676 Song X. & Barbour M.M. (2016) Leaf water oxygen isotope measurement by direct
677 equilibration. *New Phytologist* **211**, 1120-1128.

678 Song X., Barbour M.M., Farquhar G.D., Vann D.R. & Helliker B.R. (2013) Transpiration rate
679 relates to within- and across-species variations in effective path length in a leaf water
680 model of oxygen isotope enrichment. *Plant, Cell & Environment* **36**, 1338-1351.

681 Song X., Loucos K.E., Simonin K.A., Farquhar G.D. & Barbour M.M. (2015) Measurements of
682 transpiration isotopologues and leaf water to assess enrichment models in cotton. *New*
683 *Phytologist* **206**, 637-646.

684 Steudle E., Murrmann M. & Peterson C.A. (1993) Transport of water and solutes across maize
685 roots modified by puncturing the endodermis. *Plant Physiology* **103**, 335-349.

686 Strugger S. (1943) Der aufsteigende Saftsrom in der Pflanze. *Naturwissenschaft* **31**, 181-191.

687 Tomás M., Medrano H., Brugnoli E., Escalona J.M., Martorell S., Pou A., Ribas-Carbo M. &
688 Flexas J. (2014) Variability of mesophyll conductance in grapevine cultivars under water
689 stress conditions in relation to leaf anatomy and water use efficiency. *Australian Journal*
690 *of Grape Wine Research* **20**, 272-280.

691 Van Wittenberghe S., Adriaenssens S., Staelens J., Verheyen K. & Samson R. (2012) Variability
692 of stomatal conductance, leaf anatomy, and seasonal leaf wettability of young and adult
693 European beech leaves along a vertical canopy gradient. *Trees* **26**, 1427-1438.

694 Walker C.D., Leaney F.W., Dighton J.A. & Allison G.B. (1989) The influence of transpiration
695 on the equilibration of leaf water with atmospheric water vapour. *Plant, Cell &*
696 *Environment* **12**, 221- 234.

697 Welp L.P., Keeling R.F., Meijer H.A.J., Bollenbacher A.F., Piper S.C., Yoshimura K., Francey
698 R.J., Allison C.E. & Wahlen M. (2011) Interannual variability in the oxygen
699 isotopes of atmospheric $CO_2$ driven by El Nino. *Nature* **477**, 579-582.

West A.G., Patrickson S.J. & Ehleringer J.R. (2006) Water extraction times for plant and soil materials used in stable isotope analysis. *Rapid Communications in Mass Spectrometry* **20**, 1317-1321.

Yakir D., DeNiro M.J. & Rundel P.W. (1989) Isotopic inhomogeneity of leaf water: Evidence and implications for the use of isotopic signals transduced by plants. *Geochimica et Cosmochimica Acta* **53**, 2769-2773.

Zheng Y., Xu M., Shen R. & Qiu S. (2013) Effects of artificial warming on the structural, physiological, and biochemical changes of maize (*Zea mays* L.) leaves in northern China. *Acta Physiologiae Plantarum* **35**, 2891-2904.

Zwieniecki M.A., Brodribb T.J. & Holbrook N.M. (2007) Hydraulic design of leaves: insights from rehydration kinetics. *Plant, Cell & Environment* **30**, 910-921.

712 **Table 1.** List of species divided into the three hydraulic designs based on citations providing anatomical cross sections. The presence
713 (Y) or absence (N) of bundle sheath extension cells (BSE) is indicated in the labelled column. Similarly, the presence (Y) or absence
714 (N) of a significant relationship between transpiration rate and the fractional difference between the Craig-Gordon estimate for
715 evaporative enrichment and the measured bulk leaf water isotopic enrichment is indicated in the column "Péclet". Anatomical
716 notation: MR = multi-veined reticulate, MP = multi-veined paralleled, SV = single veined, P = palisade cells, S = spongy cells, Indist.
717 = indistinguishable, unstructured = no obvious mesophyll structure. For *C. sasanqua* and *W. nobilis*, more than two thirds of $1 - \Delta_L/\Delta_e$
718 were negative, thus the whole leaf Péclet effect theory used in this study is not applicable (marked N*).

| **Species** | **Vein structure** | **BSE** | **Mesophyll** | **Citation** | **Design** | **Péclet** | **Citation** |
|---|---|---|---|---|---|---|---|
| *C. sasanqua* | MR | N | P+S | John et al. 2013 | 1 | N* | Current study |
| *G. biloba* | MP | Y | unstructured | Zwieniecki et al. 2007 | 1 | N | Current study |
| *T. aestivum* | MP | N | Indist. P+S | Jahan 2016 | 1 | N | Current study |
| *V. faba* | MR | N | P+S | Current study | 1 | N, except low light and ambient $CO_2$ grown leaves | Current study |
| *C. arietinum* | MR | N | Indist. P+S | Current study | 1 | N | Current study |
| *W. nobilis* | | N | P+S | Burrows and Bullock 1999 | 1 | N* | Current study |
| 6 conifer species | | N | unstructured | Roden et al. 2015 | 1 | N | Roden et al. 2015 |
| *P. radiata* | SV | N | unstructured | Roden et al. 2009 | 1 | N | Song et al. 2013 |
| *P. rigida* | SV | N | unstructured | Bostrack and Sparrow 1969 | 1 | N | Song et al. 2013 |
| *Acer x freemanii* | MR | Y | P+S | Current study | 2 | Y | Current study |
| *E. camaldulensis* | MR | ? | P+S | Sefton et al. 2002 | 2 | Y | Current study |
| *E. globulus* | MR | Y | P+S | James et al. 1999 | 2 | Y | Current study |

| | | | | | | | |
|---|---|---|---|---|---|---|---|
| *E. grandis* | MR | Y | P+S | Sefton et al. 2002; Santos et al. 2008 | 2 | Y | Current study |
| *E. polybractea* | MR | Y | P+S | Current study | 2 | Y | Current study |
| *G. hirsutum* | MR | Y | P+S | Current study | 2 | Y | Current study |
| *P. vulgaris* | MR | Y | P+S | Morison et al. 2007, Current study | 2 | Y/N | Current study |
| ***V. vinifera* cv. Sultana M12** | MR | Y | P+S | Current study | 2 | Y | Current study |
| *A. rubrum* | MR | Y | P+S | Zwieniecki et al. 2007 | 2 | N | Song et al 2013 |
| *F. sylvatica* | | Y | P+S | Van Wittenberghe et al. 2012 | 2 | Y | Ferrio et al. 2009 |
| *V. vinifera* cv. Grenache | MR | ? | P+S | Tomás et al. 2014 | 2 | Y | Ferrio et al. 2012 |
| *E. amplifolia* | MR | Y | P only | Current study | 3 | N | Current study |
| *E. botryoides* | MR | Y | P, S? | Current study | 3 | N | Current study |
| *E. occidentalis* | MR | ? | P+S | Sefton et al. 2002 | 3 | N | Current study |
| *E. stellulata* | MR | N | Indist. P+S | Current study | 3 | N | Current study |
| *E. parramattensis* | MR | Y | Indist. P+S | Current study | 3 | N | Current study |
| *G. max* | MR | Y | Indist. P+S | Pérez Chaca et al. 2014;, Junior et al. 2009 | 3 | N | Current study |
| *H. annuus* | MR | Y | P+S | Current study | 3 | N | Current study |

719

## Figure Captions

**Figure 1.** The relationship between transpiration rate and the fractional difference between the Craig-Gordon estimate ($\Delta_e$) and measured leaf water stable oxygen isotope composition ($\Delta_L$) for the lamina and whole leaf samples of 18 species. The species are separated into the three hydraulic designs as designated in Table 1. Additionally, in panel R datasets collected in isotopic steady state and non-steady state are shown.

**Figure 2.** The relationships between transpiration rate and the fractional difference between the Craig-Gordon estimate ($\Delta_e$) and measured leaf water stable oxygen isotope composition ($\Delta_L$) for leaves of three species exposed to high (1200 μmol $m^{-2}$ $s^{-1}$; circles) and low (200 μmol $m^{-2}$ $s^{-1}$; squares) irradiance during gas exchange and transpiration isoflux measurements.

**Figure 3.** The relationship between transpiration rate and the fractional difference between the Craig-Gordon estimate ($\Delta_e$) and measured leaf water stable oxygen isotope composition ($\Delta_L$) for the major vein, lamina and composite samples of 8 selected species. The 8 species are separated into the three hydraulic designs as designated in Table 1. Note that the x-axis scale differs between panels A and B, and panels C to H.

**Figure 4**. The relationships between measured and modelled leaf water $^{18}O$ enrichment for leaves of three hydraulic designs, using the Craig-Gordon model (A) and hydraulically-informed models (B). In (B), hydraulic designs 1 and 3 use the two-pool model (Eqn 7, with an average value of $\phi$ for each species), and hydraulic design 2 leaves use the Péclet model (Eqn 12, with an average value of $L$ for each species.

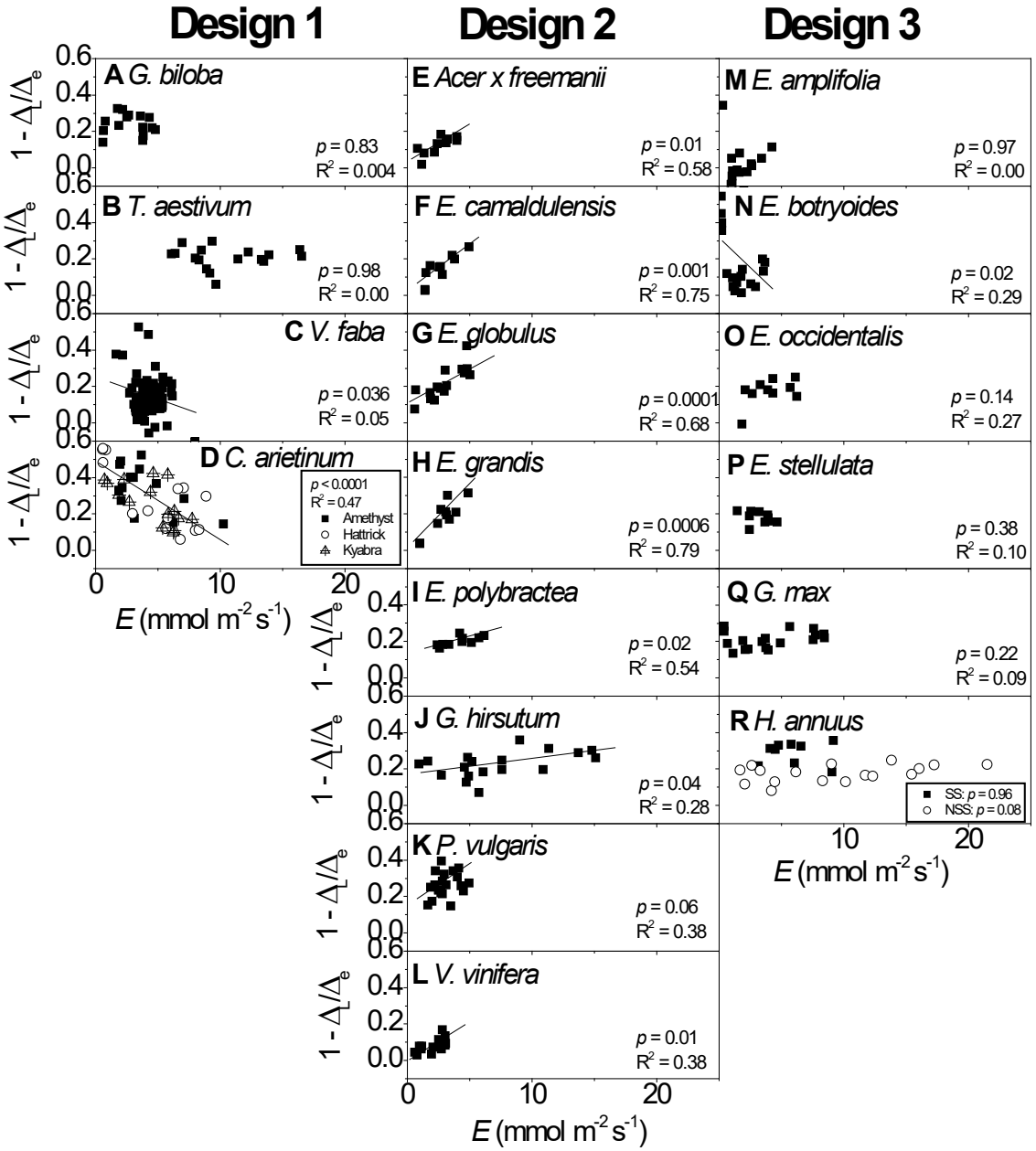
Design 1
Design 2
Design 3
A G. biloba
p = 0.83
R2 = 0.004
B T. aestivum
p = 0.98
R2 = 0.00
C V. faba
p = 0.036
R2 = 0.05
D C. arietinum
p < 0.0001
R2 = 0.47
Amethyst
Hattrick
Kyabra
E Acer x freemanii
p = 0.01
R2 = 0.58
F E. camaldulensis
p = 0.001
R2 = 0.75
G E. globulus
p = 0.0001
R2 = 0.68
H E. grandis
p = 0.0006
R2 = 0.79
I E. polybractea
p = 0.02
R2 = 0.54
J G. hirsutum
p = 0.04
R2 = 0.28
K P. vulgaris
p = 0.06
R2 = 0.38
L V. vinifera
p = 0.01
R2 = 0.38
M E. amplifolia
p = 0.97
R2 = 0.00
N E. botryoides
p = 0.02
R2 = 0.29
O E. occidentalis
p = 0.14
R2 = 0.27
P E. stellulata
p = 0.38
R2 = 0.10
Q G. max
p = 0.22
R2 = 0.09
R H. annuus
SS: p = 0.96
NSS: p = 0.08
1 - ΔL/Δe
E (mmol m-2 s-1)

Figure 1.

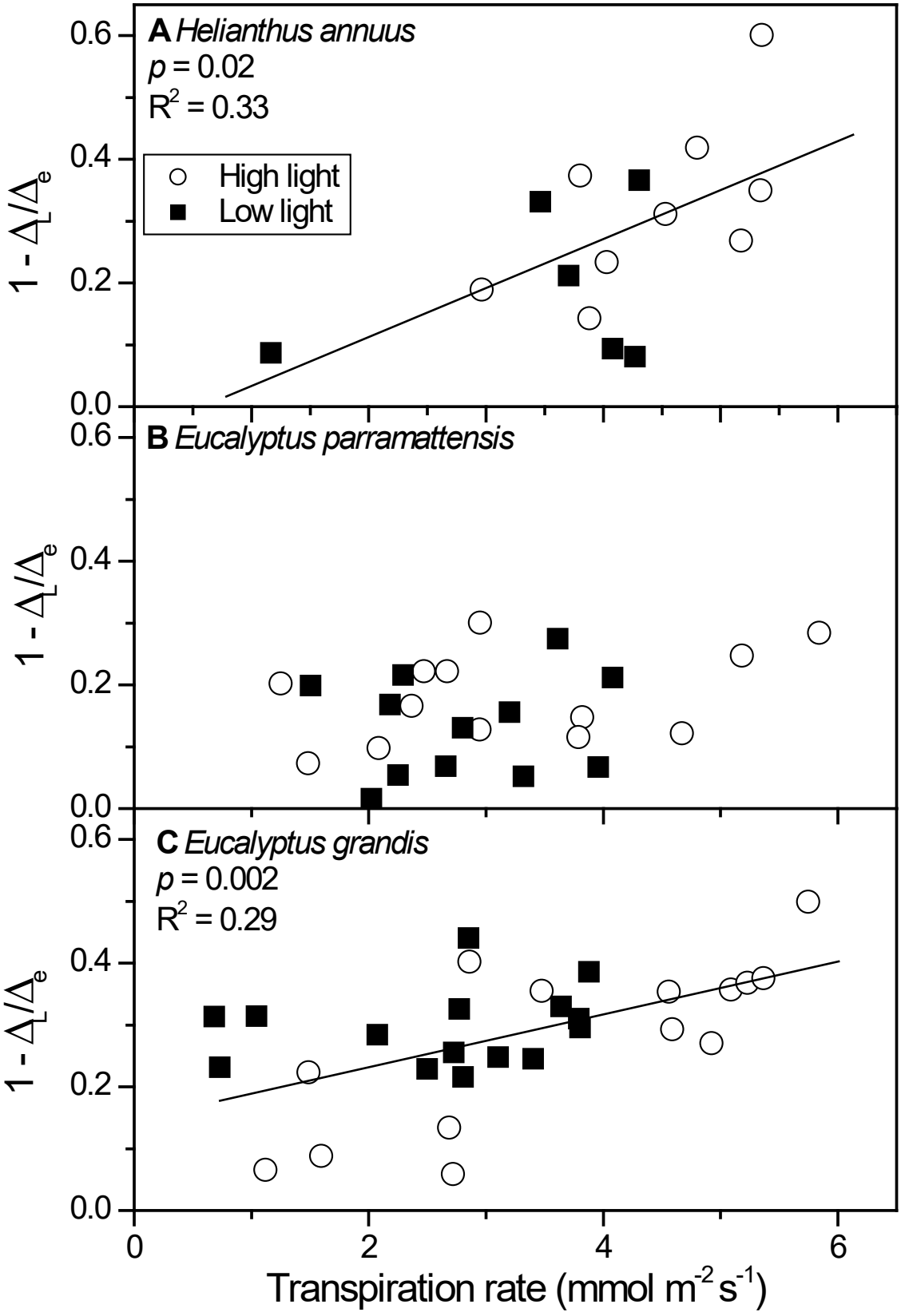
A Helianthus annuus
p = 0.02
R2 = 0.33
High light
Low light
B Eucalyptus parramattensis
C Eucalyptus grandis
p = 0.002
R2 = 0.29
1 - ΔL/Δe
0.0
0.2
0.4
0.6
0
2
4
6
Transpiration rate (mmol m-2 s-1)

Figure 2.

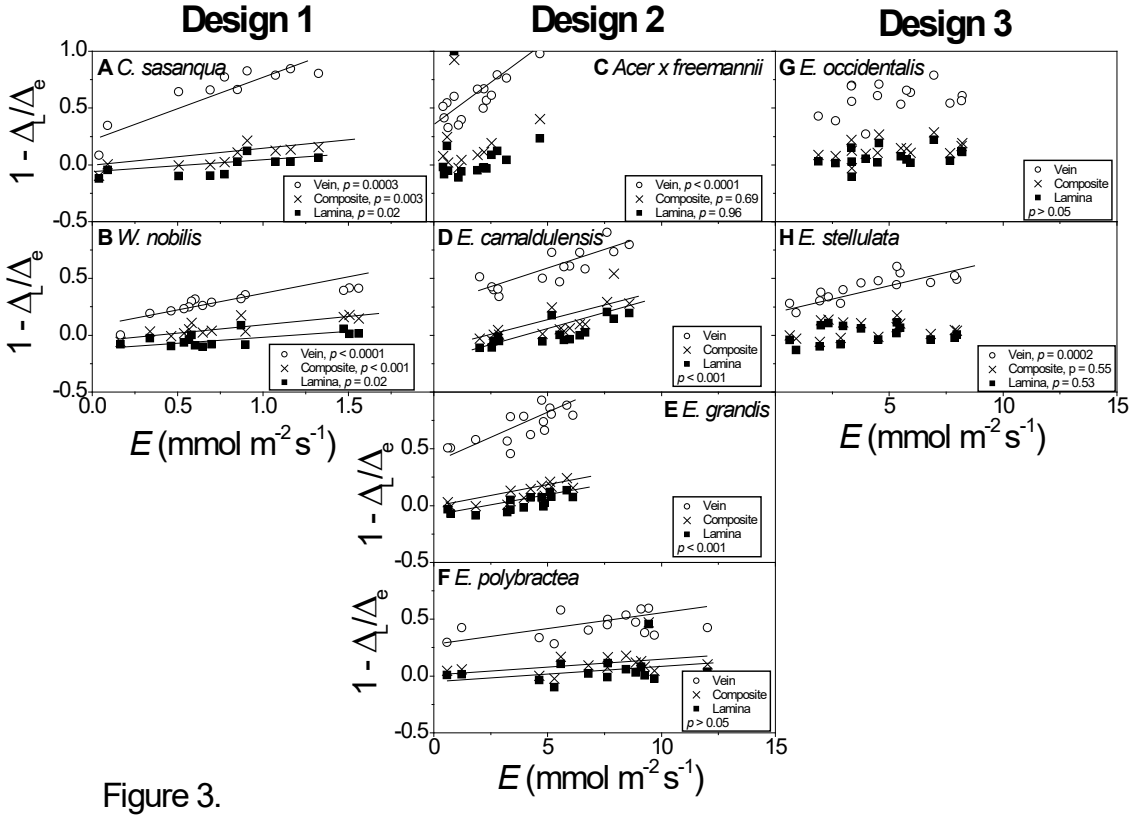
Design 1
Design 2
Design 3
A C. sasanqua
Vein, p = 0.0003
Composite, p = 0.003
Lamina, p = 0.02
C Acer x freemannii
Vein, p < 0.0001
Composite, p = 0.69
Lamina, p = 0.96
G E. occidentalis
Vein
Composite
Lamina
p > 0.05
B W. nobilis
Vein, p < 0.0001
Composite, p < 0.001
Lamina, p = 0.02
D E. camaldulensis
Vein
Composite
Lamina
p < 0.001
H E. stellulata
Vein, p = 0.0002
Composite, p = 0.55
Lamina, p = 0.53
E E. grandis
Vein
Composite
Lamina
p < 0.001
F E. polybractea
Vein
Composite
Lamina
p > 0.05
1 - ΔL/Δe
E (mmol m-2 s-1)

Figure 3.

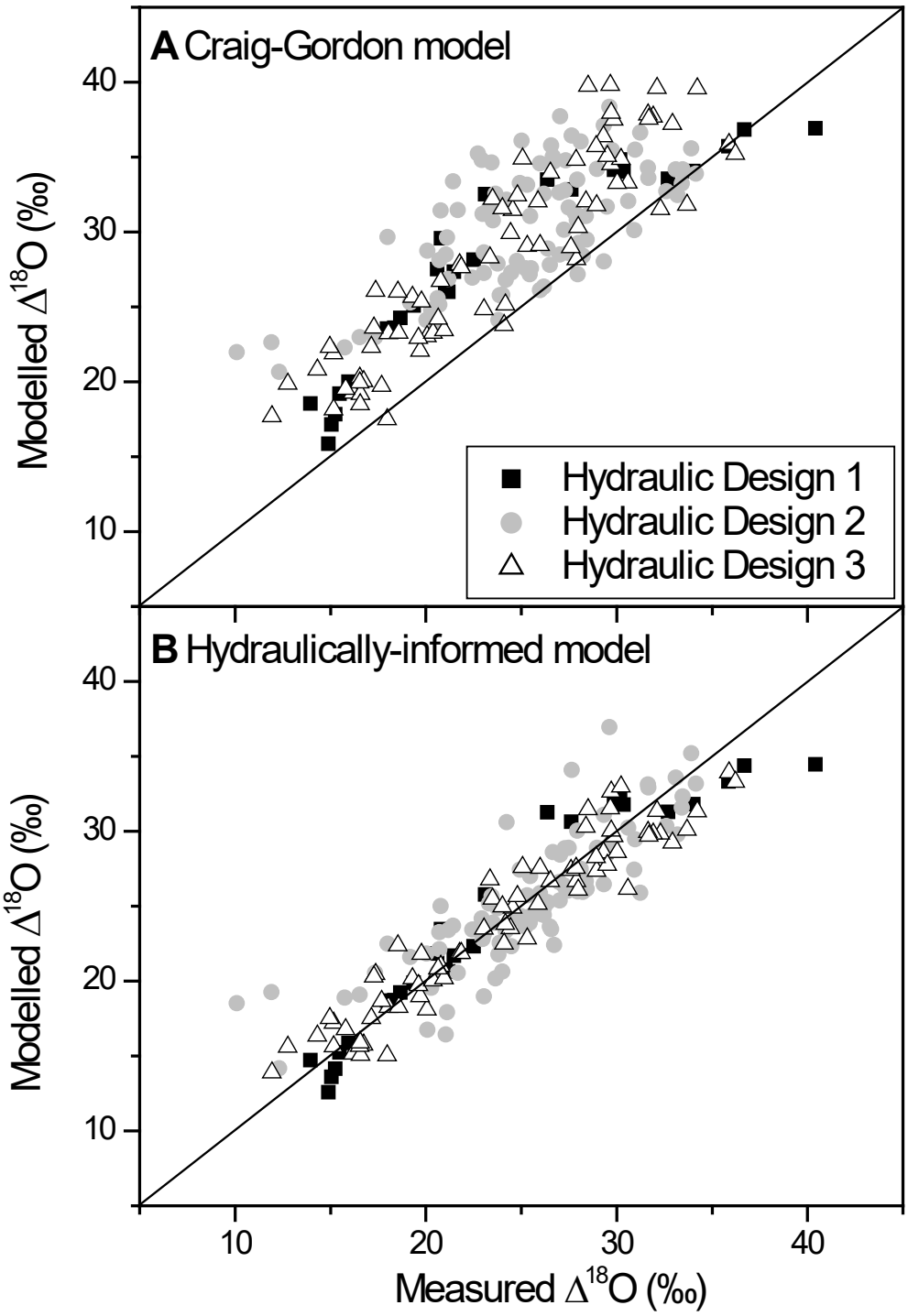
A Craig-Gordon model
B Hydraulically-informed model
Hydraulic Design 1
Hydraulic Design 2
Hydraulic Design 3
Modelled Δ18O (‰)
Measured Δ18O (‰)
10
20
30
40

Figure 4